ARTICLE

# Spotting a Conglomerate Is Just Halfway to Achieving a Preparative Resolution by Preferential Crystallization

Silvia Gonella, Julien Mahieux, Morgane Sanselme, and Gérard Coquerel*

UPRES-EA 3233, SMS, IMR 4114, Université de Rouen, Rue Lucien Tesnière, F-76 821 Mont-Saint-Aignan Cedex, France.

Ⓢ *Supporting Information*

**ABSTRACT:** Nowadays the detection of conglomerates has been improved; but with a view to implement an efficient preparative resolution by preferential crystallization, this is not enough. Indeed, when a conglomerate has been spotted, there is no other way to assess the feasibility of its preferential crystallization than to run various tests of entrainment. Three similar molecular structures in the series of 1,2-diaminocyclohexyl derivatives are presented in this work. The structures correspond to conglomerates with nonobvious stoichiometry. Two are successfully resolved by preferential crystallization; the third one cannot be resolved by entrainment.

## ■ INTRODUCTION

Enantiomers are mirror image molecules with identical chemical/physical intensive properties and opposite vectorial properties. They exhibit different properties when they are in contact with chiral environments, such as other enantiomers, living organisms, etc. As a result of these discriminative interactions, chemists have been facing an accelerating demand for chiral molecules.

Without stereoselective synthesis pathways, organic chemistry leads to an equal percentage of each enantiomer, called a racemic mixture. Because of the above-mentioned similarities, their separation is a complicated process. Therefore, the existing methods to obtain enantiomers are constantly under development and improvement to deliver a more accessible and large-scale process.[1]

Among numerous techniques to resolve racemic mixtures into enantiomers, preferential crystallization offers an efficient and cost-effective resolution process together with a quantitative yield. The resolution results from the so-called 'entrainment effect' which means that a supersaturated system in both enantiomers allows for a certain period of time the stereoselective crystallization of a single enantiomer. Unfortunately, its application is almost restricted to compounds which crystallize as stable conglomerates, i.e. a physical mixture of enantiomerically pure particles[2], i.e. no intermediate compound exists between the two antipodes.

Only ∼5% of a racemic mixture crystallizes as conglomerates. Even if this constitutes a severe limitation, no *a priori* restriction should be put when testing the associations between partners of crystallization. This means that screening of salts should be undertaken in different solvents or mixture of solvents with a view to increase the possibility of finding a conglomerate.[3,4] Moreover, regardless of the expected ratios of basic chemistry laws, the use of exotic stoichiometries can increase the occurrence.

This article aims to show the diversity in behaviour of three conglomerate-forming systems belonging to the family of symmetrical 1,2-diaminocyclohexane (DACH) derivatives. The chirality in DACH and its derivatives is in the central diamine chain as shown in Scheme 1.

Those compounds described hereafter exhibit either an unusual stoichiometry or an incongruent solubility. More specifically, this contribution illustrates the variability in preferential crystallization performances among similar chiral diamines.

## ■ RESULTS AND DISCUSSION

The racemic and enantiopure products were synthesized as described in literature[5] with the same modifications as illustrated in another paper in this issue.[6] The racemic liquid bases were used to prepare three dozens of salts in five different solvents (water, methanol, ethanol, acetone, dichloromethane) with different stoichiometries (2−1, 1−,1 and 1−2 in base−acid unit equivalents).

In order to preselect the non-centrosymmetric crystallized phases[a], SHG[7] tests were first implemented to avoid waste of time and material. Positive SHG activities led to further investigation if the racemic solid was not only non-centrosymmetric but also chiral. In order to differentiate between non-centrosymmetric and nonchiral (e.g., racemic compound with space group such as: $Pna2_1$, $Cc$, $Pca2_1$, etc.) and chiral lattices (e.g., a conglomerate) additional spectroscopic tests were carried out. As a conglomerate without partial solid solution is a physical mixture of enantiopure crystals, IR, XRPD, ssNMR, or Raman patterns of the pure enantiomer and that of the racemic mixture have to be perfectly superimposable.

The workflow applied for these salts is summarized in Scheme 2. It emphasizes that only around 10−20% of crystallized solids have to be compared with enantiopure material.

The three DACH derivatives leading to the conglomerate are shown in Figure 1. The solid phases stemming from the

pure enantiomer and the racemic mixture were compared by using XRPD.

Once a conglomerate is confirmed, efficient conditions for resolution via preferential crystallization have to be found.

As a reminder, preferential crystallization consists of alternate crystallizations of each enantiomer from supersaturated mother liquors containing initially a slight excess in a single enantiomer.[2,8] This method can be applied to every stable or metastable polymorph due to the entrainment effect conducted by kinetic factors. This means avoiding the nucleation of unwanted enantiomer during the process.

## Scheme 1. 1,2-Diaminocyclohexane (DACH) and the model derivative encountered in this study



*trans*-DACH
Commercial
racemic mixture

*Trans* enantiomeric
DACH derivatives
(100%ee)

In order to develop an efficient resolution method some specific preliminary tests have to be carried out:

- A screening of solvents so that other polymorphs or solvates can be detected *in situ*. It highlights the importance of the nature of the solvent(s) during the conglomerate screening.[8] If other crystal structures exist (examples: effluorescent solvate, metastable phase, etc.), the metastable zone,[9] the possibility of using a mixture of solvents[10] must be investigated.
- Study the solubility curve in the temperature range (in case preferential crystallization is primarily applied by cooling ramp). The temperature gap has to be chosen to avoid degradation or instability of the product in solution and allows the formation of a sufficient supersaturation between the starting ($T_B$) and the final ($T_F$) temperature of the cooling program. Other types of preferential crystallizations exist (by antisolvent addition or solvent evaporation[11]), but they are not discussed in this article.
- Adjustment of the cooling rate and the final temperature ($T_F$) so that the supersaturated solution could remain in the metastable zone. During the preferential crystallization, it prevents the spontaneous primary nucleation of the counter enantiomer which reduces the final enantiomeric excess in the crop (Ostwald's limit).[12,13]

## Scheme 2. Workflow to find a conglomerate





**Figure 1.** **2a**: *N,N′*-bis(4-chloro-benzyl)-DACH bis-hydrogenomaleate, **2b**: *N,N′*-bis-(4-bromo-benzyl)-DACH bis-dihydrogenocitrate, ethanol solvate or acetone solvate, **2c**: *N,N′*-bis-(3-piridinyl-methyl)-DACH trinitrate.
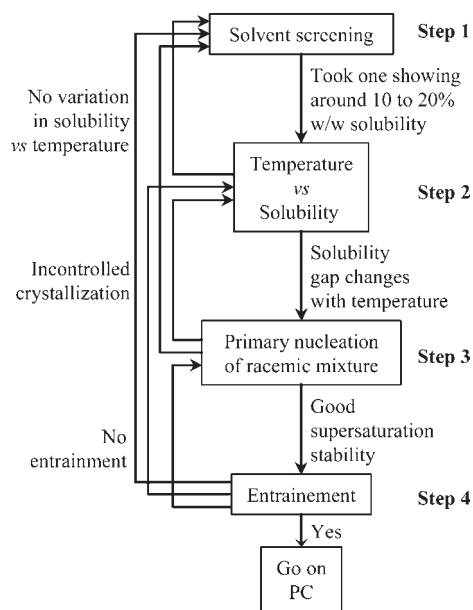
- Tuning the cooling program so that the entrainment effect is optimized. A control of the evolution of the system by optical rotation of the mother liquor or by chiral HPLC. Several problems could still appear at this step: partial solid solution,[14] epitaxy,[15] lamellar twinning[16]), slow crystallization kinetics.

These steps are summed up in Scheme 3. It highlights that sequentially each test has to be successful before going to the next one. If one test fails, the conditions of every previous stage need to be examined again and possibly modified.

Compound **2a**, [N,N'-bis(4-chloro-benzyl)DACH] bis-maleate, adheres entirely to the classical behaviour for a conglomerate in preferential crystallization. The perfect fit between XRPD patterns of racemic and enantiopure **2a** is illustrated in Figure 2.

The calculated XRPD pattern from a single crystal crystallographic data is added in order to confirm the matching of all phases and the structural purity of the solids. Figure 3 shows the first neighbours of the dibasic molecule in the crystal structure.

Four maleic acid molecules are linked by strong ionic hydrogen bonds. This unusual stoichiometry is composed of two basic functions for four acidic ones. The crystallographic parameters are detailed in Table 1.

After a solvent screening, methanol was found to give a good solubility for this salt at room temperature (Figure 4).

After a series of trial and error tests at 100-mL scale, $T_B$, $T_F$, and the cooling rate were optimized. The two-step cooling program (labelled A, hereafter) was from 45 °C ($T_B$) to 28 °C ($T_F$) in 40 min, followed by a plateau at 28 °C until filtration. The primary nucleation of the antipode appeared at 48 min, i.e. the 'filtration window' was 8 min wide.

For the very first entrainment test, an initial enantiomeric excess was added into the racemic solution at $T_B$ = 45 °C, so that the initial enantiomeric excess was ∼10%. There was then a suspension of a single enantiomer at $T_B$, providing the so-called autoseeding. The optical rotation and the refractive index of the mother liquor were monitored during the cooling program. The entrainment effect was detected by the inversion of the optical rotation sign of the mother liquor (Figure 5); 45 min seemed to correspond to the optimum duration of the stereoselective crystallization.

Five successive cycles of autoseeded polythermic programmed preferential crystallization[17] (AS3PC) were performed using the

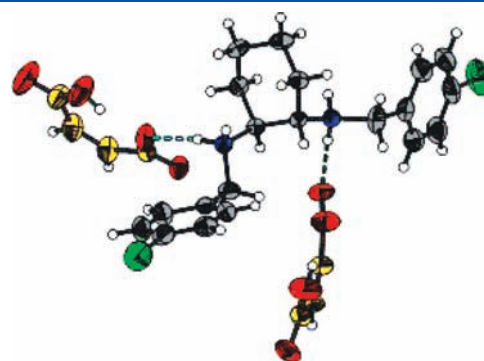**Scheme 3. Workflow for preferential crystallization conditions**

**Figure 3.** N,N'-Bis(4-chloro)diaminocyclohexane dication interacts with two half-deprotonated molecules of maleic acid. They are depicted with thermal ellipsoid representation in grey and yellow respectively. Between these three entities strong ionic hydrogen bonds are established in dashed blue lines, $d \approx 1.9$ Å.
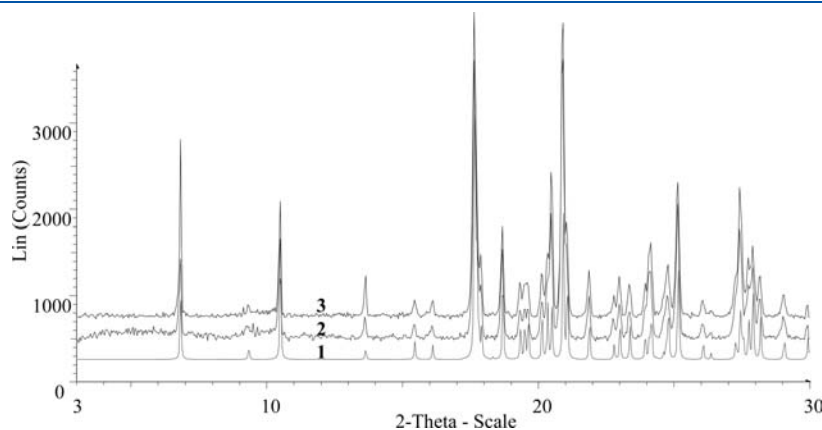
**Figure 2.** XRPD of **2a**: (1) calculated XRPD obtained by crystal structure, (2) racemic mixture, (3) enantiopure compound.

**Table 1. Crystallographic parameters of 2a and 2b**

| compound reference | 2a | 2b |
|---|---|---|
| CSD number | CCDC 819999 | CCDC 819998 |
| chemical formula | $(C_{20}H_{24}N_2Cl_2)$ $(C_4H_4O_4)_2$ | $(C_{20}H_{24}N_2Br_2)$ $(C_6H_8O_7)_2$ |
| formula mass | 595.46 | 894.56 |
| crystal system | triclinic | trigonal |
| space group | $P\bar{1}$ | $P3_112$ |
| $a$/Å | 5.7819(1) | 11.299(3) |
| $b$/Å | 9.6587(2) | 11.299(3) |
| $c$/Å | 13.317(3) | 30.405(8) |
| $\alpha$/deg | 79.109(3) | 90 |
| $\beta$/deg | 82.475(3) | 90 |
| $\gamma$/deg | 86.782(3) | 120 |
| unit cell volume/Å$^3$ | 723.7(2) | 3361.6(1) |
| calculated density | 1.366 | 1.326 |
| temperature/K | 298 | 293 |
| no. of formula units per unit cell, $Z$, $Z'$ | 1, 1 | 6, 1 |
| absorption coefficient, $\mu$/mm$^{-1}$ | 0.276 | 1.87 |
| no. of reflections measured | 5792 | 22750 |
| no. of independent reflections | 5153 | 4197 |
| no. of reflections with $I > 2\sigma I$ | 5055 | 2312 |
| $R_{int}$ | 0.0104 | 0.0588 |
| limiting indices | $h = [-7, 7]$ $k = [-12, 12]$ $l = [-15, 16]$ | $h = [-14, 13]$ $k = [-14, 13]$ $l = [-37, 37]$ |
| final $R_1$ values $(I > 2\sigma(I))$ | 0.0391 | 0.0653 |
| final $wR(F^2)$ values $(I > 2\sigma(I))$ | 0.1057 | 0.1740 |
| final $R_1$ values (all data) | 0.0398 | 0.1116 |
| final $wR(F^2)$ values (all data) | 0.1068 | 0.1840 |
| goodness of fit on $F^2$ | 1.055 | 1.210 |
| largest diff. peak and hole (e·Å$^{-3}$) | 0.404/−0.249 | 0.787/−0.358 |
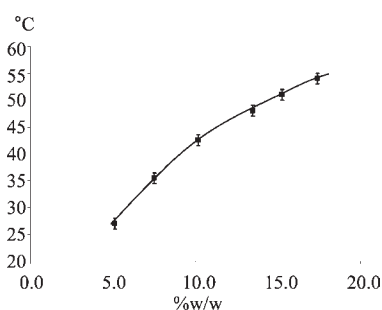


**Figure 4.** Solubility curve of racemic **2a** in MeOH.

selected cooling program A. These sets of experiments are presented in Table 2.

This preferential crystallization is reproducible (final ee standard deviation = 3.6) and with a very good optical purity (98.7%,
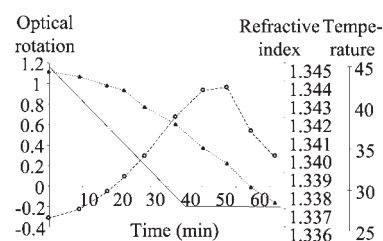


**Figure 5.** Evolution versus time of physical parameters obtained during entrainment test of **2a** in methanol. Legend: (○) = optical rotation of the mother liquor at $\lambda$ = 436 nm; (▲) = refractive index; (—) = cooling program in °C.

**Table 2. Summary of the AS3PC results for 2a**

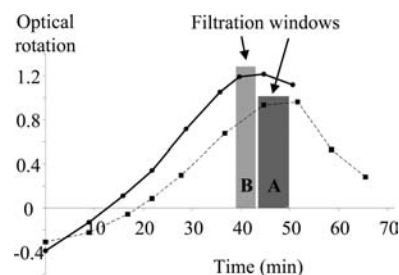| batch | duration (min) | $m_{\text{crude crops}}$ (g) | OP (%) | $m_{\text{pure crops}}$ (g) | $ee_f$ (%) |
|---|---|---|---|---|---|
| 1 | 43 | 3.94 | −69.5 | 2.74 | 21.9 |
| 2 | 43 | 3.44 | +97.1 | 3.34 | −18.8 |
| 3 | 48 | 4.46 | −98.1 | 4.37 | 23.8 |
| 4 | 50 | 4.33 | +99.6 | 4.31 | −16.1 |
| 5 | 49 | 4.36 | −99.9 | 4.36 | 22.8 |
| **average** | **47.5** | **4.15** | **±98.7** | **4.09** | **±20.4** |
| standard deviation | 3 | 0.48 | 1.3 | 0.51 | 3.6 |



**Figure 6.** Influence of the cooling program on the optical rotation of the mother liquor in the preferential crystallization of **2a**.

standard deviation = 1.3) of the raw product collected without washing and not submitted to any recrystallization.

In order to improve the productivity of the system, a different cooling program (program B): 45 to 25 °C in 30 min was applied. The ee variations versus time by using cooling programs A and B are compared in Figure 6.

The widths of the 'filtration windows' are clearly impacted by the two cooling ramps. Program B leads to a higher productivity than program A because the entrainment effect goes farther in a shorter period of time. However, program B filtration window has shrunk to such an extent that scale-up might be jeopardized.

**2b**, i.e. $N,N'$-bis(4-bromobenzyl)diaminocyclohexane bis-dihydrogenocitrate, crystallizes as a stable conglomerate in acetone. A more soluble isomorphic phase was also spotted in ethanol. A single crystal was obtained in an ethanol/acetone mixture in a slightly supersaturated solution at room temperature. The single-X-ray diffraction was carried out in a capillary to prevent the opacification of single crystals when manipulated out of mother liquor. Figure 7 represents the first neighbours of the

dication in the crystal structure. The crystallographic parameters are collected in Table 1.

The asymmetric unit is composed of one dibase molecule fully protonated, two triacid molecules monodeprotonated, and one acetone molecule. The structure was solved with one acetone
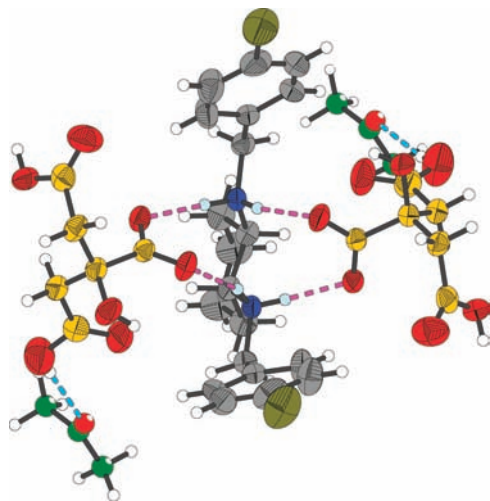


**Figure 7.** *N,N'*-Bis(4-bromobenzyl)diaminocyclohexane dication interacts with two monodeprotonated molecules of citric acid. They are depicted with thermal ellipsoid representation in grey and yellow, respectively. Between these three entities strong ionic hydrogen bonds are established in dashed pink lines, $d \approx 1.9$ Å. The solvent molecules are depicted in green and were not refined with anisotropic displacements. The solvent molecules establish strong hydrogen bonds with the protonated carboxylic moieties (depicted in dashed blue lines $d \approx 1.9$ Å).
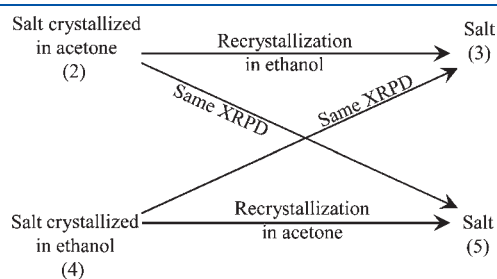


**Figure 8.** Test of isomorphism among the acetone and ethanol solvates.
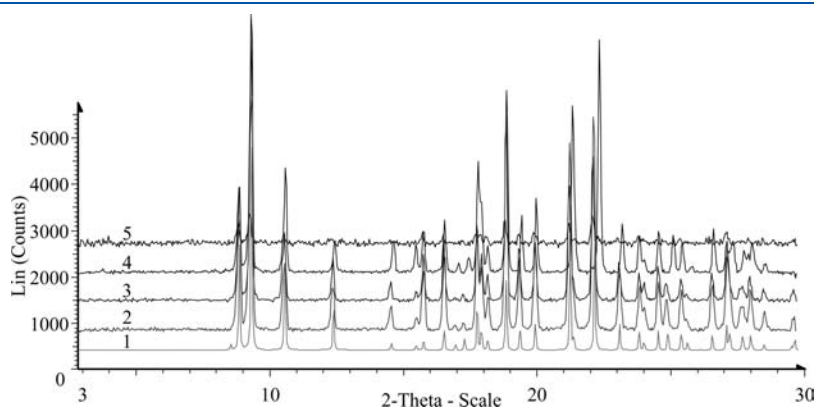
molecule, but other residual electronic density spots were remaining probably due to the mixture of solvents used for the crystal growth. However, these spots could not be assigned to any suitable molecular geometry.

Further, stability tests of the solvated phases were carried out as presented in Figure 8 with racemic and enantiopure salts. Each solvent molecule within the crystal lattice can easily be removed by the other one. According to the XRPD patterns, the main network of the structure remains unchanged. Nevertheless, slight shifts are observed. Indeed only the solvent molecules present in the crystals are exchanged.

The angular shifts within XRPD patterns between acetone and ethanol solvates can easily be detected in the range 21–23° in $2\theta$ (Figure 9).

Even if the acetone molecule is linked to the citric acid molecule by hydrogen bonds, the structure presents a partial effluorescent character at RT. A thermal treatment was applied to the acetone solvate, and the evolution of the structure is monitored by XRPD. The shifts observed at high $2\theta$ are consistent with the shortening of the crystal lattice parameters due to the acetone release. On return to RT another isomorphic phase was obtained. According to Karl Fischer analysis, this new isomorphous phase is a dihydrate.

TGA results of the three pure isomorphic solvates of **2a** are collected in Table 3. The partial effluorescent character appears as a common feature resulting from the crystal packings.

This compound presents an isomorphous crystal packing in acetone and in ethanol and even for the dihydrate after desolvation. This particularity had no real influence on the PC. However, after preliminary tests (step 4 in scheme 3), ethanol was chosen for resolution by AS3PC; indeed, in this solvent, salt **2b** exhibits the highest solubility. The solubility curve of racemic **2b** in ethanol is presented in Figure 10. The preferential crystallization has been performed at 150-mL scale.

The cooling programs A and B are reported in Table 4. The successive cycles of crystallization performed with each program are presented in Table 5.

Preferential crystallization performed by using cooling program A is reproducible (deviation$_{ee\ final}$ = 1.7) and with a good optical purity (84.2%, deviation$_{O.P.}$ = 7.7%) of the crude solid, isolated without washing or recrystallization. Process B leads to slightly higher average optical rotation but also to higher standard deviations showing the limits of instability.



**Figure 9.** Comparison between XRPD of solvate **2b**: (1) calculated of acetone solvate, (2) acetone racemic mixture solvate, (3) enantiopure of acetone solvate, (4) ethanol racemic mixture solvate, (5) hydrate racemic mixture solvate.

**Table 3. DSC data of ethanol and acetone solvates and hydrate of the enantiopure 2b salts**

| salts | $T_{onset}$ 1 (°C) | $\Delta m_{theoric}$ (%) | $\Delta m_{obs}$ (%) |
|---|---|---|---|
| acetonate | 96.7 | −6.94 | −5.42 |
| ethanolate | 88.9 | −5.51 | −4.74 |
| hydrate | 120.8 | −2.11 | −1.27 |
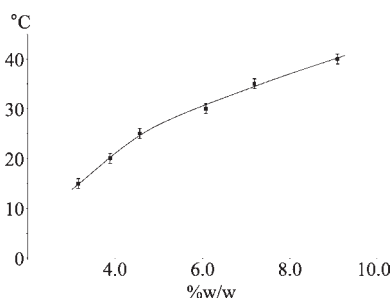


**Figure 10.** Solubility curve of racemic **2b** in ethanol.

**Table 4. Cooling programs applied to the preferential crystallization of 2b**

| program | $T_B$ (°C) | $T_F$ (°C) | time (min) | cooling rate (°C min⁻¹) | $ee_{initial}$ (%) |
|---|---|---|---|---|---|
| A | 40 | 22 | 40 | 0.45 | 3.26 |
| B | 40 | 25 | 40 | 0.37 | 4.13 |

**Table 5. Principal data of batches collected in ethanol**

| batch | duration (min) | $m_{crude\ crops}$ (g) | OP (%) | $m_{pure\ crops}$ (g) | $ee_f$ (%) | C (%) |
|---|---|---|---|---|---|---|
| 1 A | 45 | 3.289 | 98 | 3.22322 | −21.67 | 8.87 |
| 2 A | 35 | 3.54 | −75 | 2.655 | 18.23 | 9.31 |
| 3 A | 45 | 3.596 | 81 | 2.91276 | −19.79 | 10.12 |
| 4 A | 65 | 3.73 | −81 | 3.0213 | 16.77 | 9.43 |
| 5 A | 45 | 3.847 | 86 | 3.30842 | −18.35 | 10.14 |
| average | 47 | 3.600 | 84.2 | 3.024 | 19.0 | 9.574 |
| standard deviation | 10 | 0.189 | 7.7 | 0.232 | 1.7 | 0.49 |
| 1 B | 50 | 3.847 | −81 | 3.11607 | 18.47 | 3.78 |
| 2 B | 45 | 4.06 | 91 | 3.6946 | −12 | 11.76 |
| 3 B | 60 | 3.767 | −85 | 3.20195 | 16.52 | 10.93 |
| 4 B | 80 | 2.76 | 84 | 2.3184 | −12.52 | 9.55 |
| average | 59 | 3.609 | 85.3 | 3.083 | 14.9 | 9.01 |
| standard deviation | 13 | 0.501 | 3.6 | 0.493 | 2.7 | 3.12 |

The third case study is the $N,N'$-bis-(3-piridinyl-methyl)-diaminocyclohexane which crystallizes as a conglomerate with three nitric acid molecules. Although the salt was prepared with 2:1 equivalents in acid and base, respectively, the elementary analyses presented in Table 6 (left part) confirmed the unexpected stoichiometry, i.e. three molecules of acid for one molecule of dibase ($A_3B$).

**Table 6. Elementary analysis of 2c**

| | racemic mixture ($A_3B$) | | | racemic compound ($A_4B$) | | |
|---|---|---|---|---|---|---|
| | C% | H% | N% | C% | H% | N% |
| calculated | 44.54 | 5.61 | 20.20 | 39.42 | 5.15 | 20.43 |
| racemic | 44.90 | 5.65 | 20.17 | 39.74 | 5.29 | 20.89 |
| enantiopure | 44.88 | 5.68 | 20.03 | / | / | / |
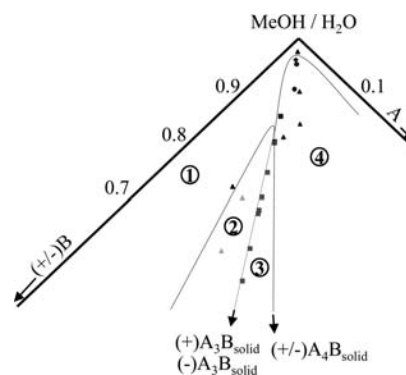


**Figure 11.** Identification by X-ray of the solid phases obtained at different compositions: ① liquid; ② (+) $A_3B_{solid}$, (−) $A_3B_{solid}$ and liquid; ③ (+) $A_3B_{solid}$, (−) $A_3B_{solid}$, (±) $A_4B_{solid}$ and liquid, ④ (±) $A_4B_{solid}$ and liquid.

During the scale-up in the preparation of a batch of racemic salt using $A_3B$ stoichiometry, a new XRPD pattern was obtained. No positive signal could be obtained in SHG; therefore, this new phase was likely to be a racemic compound. The elementary analysis gave evidence of the $A_4B$ stoichiometry (Table 6 - right part).

To understand the discrepancy between the stoichiometry applied in the preparation of the salts and the solid phases, a systematic base/acid ratio was studied by XRPD. The region of interest in the quaternary ((+)B, (−)B, A, solvent) is the isoplethal section shown in Figure 11 (MeOH/$H_2O$ ratio remains constant). The results demonstrate the noncongruent solubility of the conglomerate and the large stability region of racemic $A_4B$[18] salt.

The XRPD patterns obtained with 3:1 and 4:1 acid/base stoichiometries have been compared in Figure 12.

The racemic mixture and the pure enantiomer XRPD patterns with the $A_3B$ stoichiometry are superimposable. DSC analyses at different ee% confirm the conglomerate-forming system with the eutectic at ~180 °C. At higher temperature, these salts undergo a chemical degradation.

Due to the incongruent solubility of the conglomerate, preferential crystallization has been tested in an excess of base.[19] Thus, this system becomes a quinary system composed of <+>base, ↔ base, acid, water, and methanol. The latter component was used to limit the high solubility of the salts in water.

The solubility curve of the racemic **2c** salt was visually controlled in an excess of base (Figure 13).

Despite a careful tuning of parameters (steps 1−3), step 4 of Scheme 3 failed, i.e. no entrainment effect occurred, so the previous step was rerun with a different temperature gap. In this system another problem needed to be addressed: the A/B ratio. For A/B ≥ 3, $A_3B$ is transformed in the racemic compound $A_4B$.
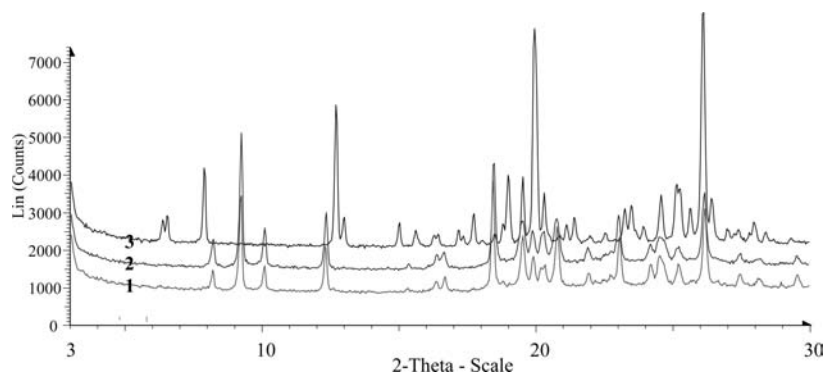
**Figure 12.** XRPD of **2c**, from bottom to top: (1) racemic mixture of $A_3B$, (2) enantiopure $A_3B$, (3) racemic compound $A_4B$.
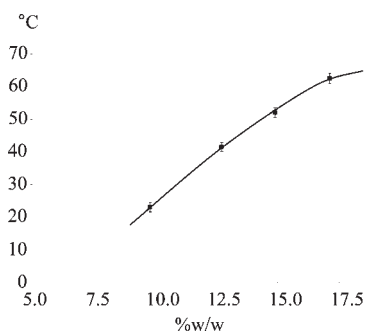


**Figure 13.** Solubility curve of the racemic mixture **2c** in base/methanol/water. A suspension with excess of base (2.6 wt % in methanol/water 75:25 wt %) was prepared and heated under stirring; when the dissolution was complete, the temperature was measured.

Conversely for $A/B \leq 2$, no solid could crystallize. Moreover, it is important to notice that the A/B ratio in the medium changes during the $A_3B$ crystallization process. Whatever the cooling rate (step 3) and the initial enantiomeric excess (step 4), no entrainment was observed for this salt.

## ■ CONCLUSION

This contribution highlights the importance of checking the nature of the solid phases directly in equilibrium with their mother liquors. Indeed, a substantial number of conglomerate-forming systems are probably missed because they only exist in suspension as an effluorescent solvate and/or as a noncongruent salt. Furthermore, this article demonstrates the interest of exploring "exotic stoichiometries" regardless of the expected ratios of basic chemistry laws.

Although spotting a conglomerate is necessary with a view to resolve the chiral mixture by PC, this is only half of the battle. A lot of phenomena can prevent a productive entrainment effect. Preliminary tests are therefore necessary because predictions are not always reliable.

Hence, time necessary to spot conglomerate-forming systems and for process design can be curtailed, but physicochemists continue to assert the lack of relationship between chiral discrimination in the solid state and the performances of preferential crystallization even in its smoothest mode, AS3PC. The predictability of PC performances is a nice subject for further research; our feeling is that the breakthrough is not in sight, but this is not a daunting prospect.

## ■ EXPERIMENTAL SECTION

**Screening Procedures for Spotting Conglomerate.** Eighty milligrams of DACH derivative racemate was weighed into 2-mL glass vials. One milliliter of solvent was added into each vial to solubilize the base, and then 2 equiv of each acid was added in the appropriate molar ratio to the quantity of the racemic mixture.

The mixtures were stirred at 20 °C for 24 h. In the case of precipitation, the solids were taken from the vials and analysed by SHG. The powders with positive signal were analysed by XRPD and compared with the enantiomeric salt prepared by using the same procedure. Identical XRPD means that a conglomerate has been spotted.

**Preferential Crystallization Experiments.** The crystallization experiments were performed at a 150-mL scale in a closed tube reactor. The temperature was controlled with a thermostat (HUBER RP 890; DT = 0.02 °C). The suspension was stirred with a magnetic bar at ~700 rpm. The process was monitored by measuring from time to time the rotatory power (polarimeter Perkin-Elmer 241) and the refractometry index (Mettler Toledo) of the mother liquor. At the chosen time, the filtration of the suspension allowed obtaining crops with high enantiopure excess. Each experiment was carried out with the characteristics (temperature, concentration, enantiomeric excess) described in the article.

**Single-Crystal X-ray Structure Determination.** A suitable single crystal of **2a** was obtained by slow evaporation of a saturated solution in methanol at room temperature. A single crystal of **2b** was obtained by a solution in 1:3 wt ethanol/acetone mixture saturated at 30 °C and then cooled at room temperature.

The crystal structures were determined from single-crystal diffraction on a SMART APEX diffractometer (with Mo K$\alpha_1$ radiation: $\lambda$ = 0.71073 Å). The structures were solved by direct methods (SHEL-XS[20]). Anisotropic displacement parameters were refined for all non-hydrogen atoms using SHEL-XL available with the WinGX package. All hydrogen atoms were included in the models in calculated positions and were refined as contained to bonding atoms.

For **2a**, the final cycle of full-matrix least-squares refinement on $F^2$ was based on 5153 observed reflections and 363 variable parameters and converged with unweighted and weighted agreement factors of $R_1$ = 0.0387, $wR_2$ = 0.1023 for 5055 reflections with $I > \sigma I$ and $R_1$ = 0.0394, $wR_2$ = 0.1033 for all data (see Table 1).

For **2b**, the final cycle of full-matrix least-squares refinement on $F^2$ was based on 4197 observed reflections and 250 variable

parameters and converged with unweighted and weighted agreement factors of $R_1 = 0.0503$, $wR_2 = 0.1167$ for 2312 reflections with $I > 2\sigma I$ and $R_1 = 0.0977$, $wR_2 = 0.1310$ for all data (see Table 1).

## ■ ASSOCIATED CONTENT

**ⓢ Supporting Information.** Additional CIF data for the crystal structures described. This material is available free of charge via the Internet at http://pubs.acs.org

## ■ AUTHOR INFORMATION

**Corresponding Author**
Fax: +33 (0) 2 35 52 29 27. E-mail: gerard.coquerel@univ-rouen.fr.

## ■ ACKNOWLEDGMENT

## ■ ADDITIONAL NOTE

[a] A large majority of racemic compounds is centrosymmetric.

## ■ REFERENCES

(1) Jacques, J.; Collet, A.; Wilen, S. H. *Enantiomers, Racemates, and Resolutions*; :Krieger: Malabar, Fla, 1994.

(2) Coquerel, G. *Novel Optical Resolution Technologies*; Springer: Berlin/Heidelberg, 2007; p 1.

(3) Tauvel, G.; Sanselme, M.; Coste-Leconte, S.; Petit, S.; Coquerel, G. *J. Mol. Struct.* **2009**, *936*, 60.

(4) Wermester, N.; Lambert, O.; Coquerel, G. *CrystEngComm* **2008**, *10*, 724.

(5) Jones, M. D.; Mahon, M. F. *J. Organomet. Chem.* **2008**, *693*, 2377.

(6) Zgonnik, V.; Gonella, S.; Mazières, M. R.; Guillen, F.; Coquerel, G.; Plaquevent, J. C. *Org. Process Res. Dev.* **2012** 10.1021/op200082a.

(7) Galland, A.; Dupray, V.; Berton, B.; Morin-Grognet, S.; Sanselme, M.; Atmani, H.; Coquerel, G. *Cryst. Growth Des.* **2009**, *9*, 2713.

(8) Coquerel, G.; Amabilino, D.B. The Nanoscale Aspects of Chirality in Crystal Growth: Structure and Heterogeneous Equilibria. In *Chirality at the Nanoscale: Nanoparticles, Surfaces, Materials and More*; Amabilino, D. B., Ed.; Wiley-VCH: Weinheim, Germany, 2009; Chapter 10.

(9) Courvoisier, L.; Mignot, L.; Petit, M. N.; Coquerel, G. *Org. Process Res. Dev.* **2003**, *7*, 1007.

(10) Wacharine-Antar, S.; Levilain, G.; Dupray, V.; Coquerel, G. *Org. Process Res. Dev.* **2010**, *14*, 1358.

(11) Levilain, G.; Coquerel, G., submitted patent

(12) Ostwald, W. *Phys. Z. Chem* **1897**, 289.

(13) Ting, H. H.; McCabe, W. L. *Ind. Eng. Chem.* **1934**, *26*, 1201.

(14) Renou, L.; Morelli, T.; Coste, S.; Petit, M. N.; Berton, B.; Malandain, J. J.; Coquerel, G. *Cryst. Growth Des.* **2007**, *7*, 1599.

(15) Gervais, C.; Beilles, S.; Cardinael, P.; Petit, S.; Coquerel, G. *J. Phys. Chem. B* **2002**, *106*, 646.

(16) Pauchet, M.; Morelli, T.; Coste, S.; Malandain, J. J.; Coquerel, G. *Cryst. Growth Des.* **2006**, *6*, 1881.

(17) Coquerel, G.; M. N. Petit, Bouaziz, R. (University of Rouen, Mont-Saint Aignan, FR). WO/95/08522, 1995.

(18) Ricci, J. E. *The Phase Rule and Heterogeneous Equilibrium*; Dover Inc.: New York, 1966.

(19) Coquerel, G.; Petit, M. N.; Bouaziz, R. *Chirality* **1992**, *4*, 400.

(20) Sheldrick, G. *Acta Crystallogr., Sect. A* **1990**, *46*, 467.